

AD-A119 384

CALIFORNIA INST OF TECH PASADENA ARTHUR AMOS NOYES L--ETC F/G 20/8  
DYNAMICS OF HYDROGEN ATOM AND PROTON TRANSFER REACTIONS. NEARLY--ETC(U)  
SEP 82 V BABAMOV, Y LOPEZ, R A MARCUS N00014-79-C-0009

UNCLASSIFIED

CONTRIB-6726

NL

1 of 1  
AD-A  
119384

END

DATE

FILED

10-82

DTIC

12

SECURITY CLASSIFICATION OF THIS PAGE (When Data Entered)

REPORT DOCUMENTATION PAGE		READ INSTRUCTIONS BEFORE COMPLETING FORM
1. REPORT NUMBER 12	2. GOVT ACCESSION NO. AD-A119384	3. RECIPIENT'S CATALOG NUMBER
4. TITLE (and Subtitle) Dynamics of Hydrogen Atom and Proton Transfer Reaction. Nearly Degenerate Asymmetric Case.		5. TYPE OF REPORT & PERIOD COVERED Technical Report
7. AUTHOR(s) V. Babamov, V. Lopez and R. A. Marcus		6. PERFORMING ORG. REPORT NUMBER
8. PERFORMING ORGANIZATION NAME AND ADDRESS Noyes Chemical Laboratory California Institute of Technology Pasadena, California 91125		9. CONTRACT OR GRANT NUMBER(s) N 000 14 - 79 - 0009
11. CONTROLLING OFFICE NAME AND ADDRESS Office of Naval Research Chemistry Program Arlington, VA 22217		10. PROGRAM ELEMENT, PROJECT, TASK AREA & WORK UNIT NUMBERS Task No. NR 359-702
14. MONITORING AGENCY NAME & ADDRESS (if different from Controlling Office)		12. REPORT DATE September 9, 1982
		13. NUMBER OF PAGES 30
		15. SECURITY CLASS. (of this report)
		15a. DECLASSIFICATION/DOWNGRADING SCHEDULE
16. DISTRIBUTION STATEMENT (of this Report) This document has been approved for public release and sale; its distribution is unlimited.		
17. DISTRIBUTION STATEMENT (of the abstract entered in Block 20, if different from Report)		
18. SUPPLEMENTARY NOTES Prepared for publication in the Journal of Chemical Physics.		
19. KEY WORDS (Continue on reverse side if necessary and identify by block number) Atom transfers; symmetric reaction; tunneling. yields		
20. ABSTRACT (Continue on reverse side if necessary and identify by block number) A method for approximate treatment of collinear H-atom or proton transfer reactions $AH + B \rightarrow A + HB$ which involve two nearly degenerate vibrational states is developed. The method is based on constructing a diabatic representation of the problem, i.e. one in which the reactant and the product vibrational states are distinguished as such throughout the collision. The diabatic representation is constructed with the aid of the adiabatic out discussed in an earlier paper. The treatment can also be applied to symmetric exchange reactions in which case it gives results in good agreement with other results.		

DTIC  
SELECTED  
SEP 20 1982  
H

AD A119384

DTIC FILE COPY

DD FORM 1 JAN 73 1473

EDITION OF 1 NOV 65 IS OBSOLETE  
S/N 0102-LP-014-6601

Unclassified

SECURITY CLASSIFICATION OF THIS PAGE (When Data Entered)

82

021

DYNAMICS OF HYDROGEN ATOM AND PROTON TRANSFER REACTIONS.  
NEARLY DEGENERATE ASYMMETRIC CASE.

V. Babamov  
Centro de Graduados  
Instituto Tecnológico de Tijuana  
Apdo Postal 1166  
Tijuana, B.C., Mexico

V. Lopez and R. A. Marcus  
Noyes Laboratory of Chemical Physics  
California Institute of Technology  
Pasadena, California 91125

Contribution No. 6726

## ABSTRACT

A method for approximate treatment of collinear H-atom or proton transfer reactions  $AH + B \rightarrow A + HB$  which involve two nearly degenerate vibrational states is developed. The method is based on constructing a diabatic representation of the problem, i.e. one in which the reactant and the product vibrational states are distinguished as such throughout the collision. The diabatic representation is constructed with the aid of the adiabatic one discussed in an earlier paper.

The treatment can also be applied to symmetric exchange reactions, in which case it yields good agreement with other results.



Accession For	
NTIS GRA&I	<input checked="checked" type="checkbox"/>
DTIC TAB	<input type="checkbox"/>
Unannounced	<input type="checkbox"/>
Justification	
By	
Distribution/	
Availability Codes	
Dist	Avail and/or Special
A	

## I. INTRODUCTION

In an earlier paper<sup>1</sup>, henceforth referred to as I, a simplified approximate treatment of symmetric collinear reactions in which an H-atom or a proton is transferred between two heavier particles was developed. The treatment was based on the adiabatic near separability of the faster H-atom motion from the slower relative motion of the heavy particles. It was useful to employ polar coordinates: The radial coordinate represents the translational motion of the heavier particles and the angular coordinate corresponds to the vibrational motion of the H-atom.

Due to the exact degeneracy of the vibrational motion of the reactants and the products the adiabatic vibrational states are symmetric and antisymmetric linear combinations of the reactants' and products' vibrational states, which are exactly decoupled by symmetry. As a result, the reactive transition probabilities between states with the same vibrational quantum number can be evaluated approximately within the adiabatic approximation.

There have been some accurate numerical calculations on collinear H-atom transfer reactions since the publication of I which provide an opportunity to test the validity of the approximations used there. The comparisons of the results of the accurate numerical calculations with those of I are presented in Sec. 2. A somewhat different approach to the symmetric H-atom exchange, which has the advantage of being more readily extendable to the nonsymmetric case is also developed and tested in Sec. 3.

The transfer of an H-atom in an asymmetric reaction is considerably more difficult to treat. Unlike in the symmetric case, the reactant and product states are no longer exactly degenerate and the reaction can occur only as a result of a breakdown of the adiabatic approximation. Consequently, two or more

coupled vibrational states are generally involved in the dynamics and approximate solutions to a set of coupled equations must be developed.

Reasonably good analytical approximations to the reaction probability over a wide energy range can be developed only in the case when the problem can be reduced to the interaction of only two coupled vibrational states, the initial reactant state and the final product state, namely when they are nearly degenerate. This is the case which is treated in the remainder of the paper.

The procedure used in the paper to treat the above problem is the following:

1. The diagonal elements of the equations in the adiabatic representation are first obtained using the procedure described in I.
2. The diabatic equations are then obtained in an approximate way utilizing the above-mentioned adiabatic ones (a) for the case of strong and moderate coupling and (b) (semiclassically) for the case of very weak coupling (Sec. 4).
3. The transition probability is finally obtained from the coupled diabatic equations using an exponential DWBA approximation.

The reason for step 1 is that the coupled adiabatic equations in terms of polar coordinates constitute a very compact representation<sup>1-3</sup> of the system. The reason for going through step 2 is that a simple analytic approximation to the solution of two coupled equations can most readily be obtained in the diabatic representation.

A perturbative (DWBA) method for solving the diabatic equations in the weak coupling limit and a procedure for extending the validity of the results to cases of higher coupling are then used (Sec. 5) to obtain the transition probabilities.

Numerical results are presented in Sec. 6.

## II. SYMMETRIC H-ATOM EXCHANGE. COMPARISON WITH ACCURATE NUMERICAL RESULTS.

It was shown in I that the Schrodinger equation for a collinear H-atom transfer collision can be transformed into a set of coupled ordinary differential equations in the adiabatic representation:

$$\left[ -\frac{1}{2} \frac{d^2}{d\rho^2} - (E - \epsilon_i + \frac{1}{8\rho^2}) \right] \phi_i(\rho) + \sum_j (-1P_{ij} \frac{d}{d\rho} + \frac{1}{2} Q_{ij}) \phi_j(\rho) = 0 \quad (2.1)$$

The symbols are defined in I. It was also shown that for a symmetric system the reactive transition probability without a change in vibrational quantum number  $P_{00}^R$  can be obtained from the elastic collision phase shifts for the two lowest states of Eq. (2.1). Those states satisfy

$$\left[ -\frac{1}{2} \frac{d^2}{d\rho^2} + \epsilon_0^s(\rho) \right] \phi_0^s(\rho) = E \phi_0^s(\rho) \quad (2.2a)$$

$$\left[ -\frac{1}{2} \frac{d^2}{d\rho^2} + \epsilon_0^a(\rho) \right] \phi_0^a(\rho) = E \phi_0^a(\rho) \quad (2.2b)$$

which are exactly decoupled by symmetry.  $P_{00}^R$  is given by:

$$P_{00}^R = |S_{00}^R|^2 = \sin^2(\xi_0^s - \xi_0^a) \quad (2.3)$$

where  $\xi_0^s$  and  $\xi_0^a$  are the phase shifts for eq. (2.2a) and (2.2b), respectively.

There have been some accurate numerical calculations on collinear H-atom transfer reactions since the publication of I, namely for the  $IH + I$  and  $I + \mu I$  systems<sup>3,4</sup> which enables us to test the accuracy of the approximation developed in I. Fig. (1) shows the comparison of the results of Eq. (2.3) and of the accurate numerical calculation<sup>3</sup> for the  $IHI$  system. It can be seen that if the mass of the end atoms is sufficiently greater than the mass of the center atom, the results are practically identical with the results of the accurate numerical calculations.

The only difference in the case of the  $IHI$  system<sup>3</sup> is that the  $P_{00}^R$  vs. energy curve obtained from eq. (2.3) is shifted by  $\sim 0.5 \cdot 10^{-4}$  kcal toward the lower energies in respect to the accurate numerical results<sup>5</sup>. Such shifts were also discussed in I and are roughly proportional to the ratio of the masses of the end and the middle atom. For the  $I\mu I$  system the corresponding shift can be expected to be about an order of magnitude smaller, which is most likely well within the limits of accuracy<sup>6</sup> of the numerical calculation<sup>4</sup>.

Eq. (2.2) is, as confirmed by the agreement in Fig. 1., a very convenient one for evaluating the ground state reaction transition probabilities for a symmetric H-atom exchange reaction.

This treatment, however, can not be directly generalized to an asymmetric system which lacks the symmetry basis for the decoupling. To facilitate the extension to the asymmetric case, another two state approximation, one in the so-called diabatic representation, will be developed and tested in the remainder of this section. Since in the two state approximation (Eq. 2.2) the set of coupled adiabatic equations (Eq. 2.1) for a symmetric system is exactly solvable, its solution is used to check the accuracy of the alternate diabatic approach, for which it constitutes the starting point.



### III. DIABATIC TREATMENT OF THE SYMMETRIC CASE

The equations in the diabatic representation are the equations for the  $\rho$ -dependent coefficient in an expansion of the wave function in the form

$$\psi(s;\rho) = \sum_i \psi_i(\rho) \eta_i(s;\rho) \quad (2.4)$$

where  $\eta_i(s;\rho)$  are  $s$ -dependent vibrational wave functions<sup>7</sup> with a weak parametric dependence on  $\rho$ . They can be written in a matrix form as:

$$\left[ -\frac{1}{2} \frac{d^2}{d\rho^2} + \underline{\underline{V}}(\rho) \right] \underline{\underline{\psi}}(\rho) = E \underline{\underline{\psi}}(\rho) \quad (3.2)$$

where  $\underline{\underline{V}}(\rho)$  is a Hermitian matrix whose elements  $V_{ij}$  are all scalars, i.e. do not contain any derivatives, and  $\underline{\underline{\psi}}(\rho)$  is a column vector with elements  $\psi_i(\rho)$ .

A set of coupled equations in the adiabatic representation can, in general, be transformed into the diabatic representation by finding a transformation matrix  $\underline{\underline{T}}$  acting on the solution wave function vector  $\phi$ :

$$\underline{\underline{\psi}} = \underline{\underline{T}} \phi \quad (3.3)$$

$\underline{\underline{T}}$  is given by the solution of the differential equation:

$$p \underline{\underline{T}} = \underline{\underline{P}} \underline{\underline{T}} \quad (3.4)$$

where  $p$  is the momentum operator  $p = -i\hbar \frac{d}{d\rho}$  and  $\underline{\underline{P}}$  is the kinetic coupling

matrix with elements  $P_{ij}$  in the set of coupled equations in the adiabatic representation. The appropriate boundary condition for the equation in the diabatic representation is that  $\underline{\psi}$  reduces to the properly separable asymptotic translational wave function at large  $\rho$ .

In the particular case of (2.2), the coupling matrix  $\underline{P}$  in (2.2) vanishes because of symmetry. The solution of (3.4), namely  $\underline{I} = \text{const.}$ , is then trivial, the value of the constant matrix  $\underline{I}$  being

$$\underline{I} = \frac{1}{\sqrt{2}} \begin{pmatrix} 1 & 1 \\ 1 & -1 \end{pmatrix} \quad (3.5)$$

since at large  $\rho$   $\phi^S$  and  $\phi^A$  are symmetric and antisymmetric linear combinations of the proper asymptotic states. The transformation (3.3), with  $\underline{I}$  given by (3.5), transforms (2.2) into the form (3.2), namely:

$$\left( -\frac{1}{2} \frac{d^2}{d\rho^2} + V_{11}(\rho) - E \right) \psi_1(\rho) = -V_{12} \psi_2(\rho) \quad (3.6)$$

$$\left( -\frac{1}{2} \frac{d^2}{d\rho^2} + V_{22}(\rho) - E \right) \psi_2(\rho) = -V_{21} \psi_1(\rho)$$

where

$$V_{11} = V_{22} = \epsilon^+; \quad \epsilon^+ = \frac{\epsilon_1 + \epsilon_2}{2} \quad (3.7a)$$

$$V_{12} = V_{21} = \epsilon^-; \quad \epsilon^- = \frac{\epsilon_2 - \epsilon_1}{2} \quad (3.7b)$$

Solving the coupled equations (3.6) numerically would, of course, give the same results already given by Eq. (2.3). Eq. (3.6) can also be solved perturbationally yielding what is usually known as the DWBA<sup>9</sup> solution for the transition matrix element:

$$T_{12}^0 = \int_0^\infty \psi_1^0(\rho) V_{12}(\rho) \psi_2^0(\rho) d\rho \quad (3.8)$$

where  $\psi_i^0(\rho)$  are the solutions of the analogs Eq. (3.6) with the r.h.s., i.e. the coupling  $V_{12}$  set to zero. Linearizing the  $V_{ij}$  and the exponent of  $V_{12}$ ,  $\alpha$ , ( $= -\ln V_{12}$ ) around the turning point, one can evaluate the integral (3.8) analytically to yield (c.f. Sec. V):

$$|S_{12}|^{\frac{1}{2}} = 2\pi T_{12}^0 = \frac{V_{12}^0}{(\alpha F)^{\frac{1}{2}}} e^{\frac{\alpha^3}{12\pi^3}} \quad (3.9)$$

Eq. (3.9) differs from the semiclassical result (5.11) in I only by the exponential factor in (3.9), which is in most cases very close to unity. A more accurate, albeit more complicated, analytic approximation to (3.8) than (3.9) also exists<sup>10</sup>. For the present purposes, however, the simpler expression (3.9) is sufficiently accurate.

The perturbative DWBA expression (Eq. 3.8) is valid only in the weak coupling case ( $\psi \approx \psi_1^0, |T_{12}|^2 \ll 1$ ). It can, however, be readily extended to the case of higher coupling (i.e., higher transition probabilities) by introducing in an ad hoc way the sinusoidal dependence of the transition probability

$$p_{00}^R = \sin^2(2\pi T_{12}^0) , \quad (3.10)$$

known as the exponential DWBA approximation.<sup>11</sup>

The transition probability vs. energy obtained from Eq. (3.9) and (3.10) is shown in Fig. 2, together with the exact solution of E. (2.2) given by Eq. (2.3). The logarithm of the transition probability vs. energy in the tunneling region, obtained from Eq. (3.10) and from (2.3), is shown in Fig. 3.

The surface used is a LEPS surface with the asymptotic parameters being those of the  $IH + I \rightarrow I + HI$  reaction.<sup>12</sup> Its potential energy contour plot is shown in Fig. 4.

It is seen from Figs. 2 and 3 that the exponential DWBA approximation to the result of the coupled equations in the diabatic representation yields for the symmetric case a result in satisfactory agreement with the exact result (Eq. 2.3). The exponential DWBA approximation to the solution of a pair of coupled equations can, therefore, be assumed to give a good approximation to their solution.

In the next section, a procedure for obtaining a pair of coupled equations in the diabatic representation for a nearly degenerate asymmetric H-atom exchange problem is developed.

#### IV. THE NEARLY DEGENERATE H-ATOM TRANSFER. GENERATING THE DIABATIC REPRESENTATION.

(a) Moderate to strong coupling.

We consider the case where two of the adiabatic diagonal terms in Eq. (2.1), one of which asymptotically corresponds to a reactant state and the other to a

product state, are nearly degenerate at large values of  $\rho$ . The nature of the interaction between such two states is closely related to that between two states which have the same quantum number in a symmetric system. For the nearly degenerate case, the following closely related approximate treatment is developed.

First, the adiabatic eigenvalues are calculated, either quantum mechanically as described in I, or if one prefers less computation at a slight loss of accuracy, from a semiclassical treatment of a double minimum potential.<sup>13</sup>

The most important simplification arises from the fact that the two nearly degenerate states interact much more strongly with each other than with the other states of the system, and the interaction with the other states can be neglected. The problem can hence be reduced to interaction of two states, a case particularly amenable to an approximate solution.

Upon neglecting all but the two nearly degenerate states, Eq. (2.1) reduces to

$$\begin{aligned} \left[ -\frac{1}{2} \frac{d^2}{d\rho^2} + \epsilon_1 - \frac{1}{8\rho^2} - E + Q_{11} \right] \phi_1(\rho) &= i P_{12} \frac{d}{d\rho} \phi_2(\rho) \\ \left[ -\frac{1}{2} \frac{d^2}{d\rho^2} + \epsilon_2 - \frac{1}{8\rho^2} - E + Q_{22} \right] \phi_2(\rho) &= i P_{21} \frac{d}{d\rho} \phi_1(\rho) \end{aligned} \quad (4.1)$$

An example for which such near-degeneracy occurs is the  $\text{ClH} + \text{Br} \rightarrow \text{Cl} + \text{HBr}$  reaction.<sup>12</sup> A contour plot for a model LEPS surface with the asymptotic

parameters such as to fit the above reactions is shown on Fig. 6. The diagonal elements of Eq. (4.1) for this surface are shown in Fig. 7 with the dashed lines.

The usual method for transforming from an adiabatic to a diabatic representation by diagonalizing the kinetic energy matrix can generally not be used when there is a transfer of a particle involved, except in the somewhat trivial case of Eq. (2.2) where the kinetic coupling matrix vanishes. The reason is that a part of the parametric dependence of the basis set  $\chi(s;\rho)$ , and consequently, of the kinetic coupling, is an artifact of the way in which the  $\chi(s;\rho)$  are defined and does not correspond to an actual interaction of the underlying diabatic states. This problem appears frequently in electron transfer reactions and is known as the translation factor problem.<sup>14,15</sup> Another way of determining the diabatic matrix elements  $V_{11}$ ,  $V_{22}$  and  $V_{12}$  which does not make use of the nonadiabatic coupling element needs to be devised.

The diagonalization condition for a two state diabatic potential energy matrix can be written as

$$\epsilon_{1,2} = \frac{V_{11} + V_{22}}{2} \pm \sqrt{\left(\frac{V_{22} - V_{11}}{2}\right)^2 + V_{12}^2} \quad (4.2)$$

or, in a form more convenient for our purposes in terms of  $\epsilon^+$  and  $V^+$ , as

$$\epsilon^+ = \frac{\epsilon_{11} + \epsilon_{22}}{2} ; \quad V^+ = \frac{V_{11} + V_{22}}{2} . \quad (4.3)$$

One finds from Eq. (4.2) that

$$V^+ = \epsilon^+ \quad (4.4)$$

and

$$H_{12}^2 = (\epsilon^-)^2 - (V^-)^2 \quad (4.5)$$

That is, the sum of the two diabatic diagonal terms equals the sum of the adiabatic ones in the two state approximation. However, in order to obtain the diabatic interaction matrix element  $V_{12}$  (Eq. 4.5), as well as the individual diagonal diabatic elements  $V_{11}$  (Eq. 4.3), the difference between the diagonal diabatic matrix element for the two states involves must be known.

It can be assumed on physical grounds that the diabatic vibrational states, which in general can be identified with a particular configuration throughout the collision, are associated with one of the wells of the double well potential (Fig. 6). Eigenstates localized in a single well can be defined in a multitude of ways: These eigenvalues will generally be somewhat sensitive to the choice and cannot be readily identified with the diabatic states' eigenvalues. The difference between the single well eigenvalues is substantially less sensitive to that choice and will be assumed to approximate fairly closely the difference between the diabatic eigenvalues. Accordingly, we make the approximation

$$V^- \approx \frac{E_2^0 - E_1^0}{2} \quad (4.6)$$

where  $E_1^0$  and  $E_2^0$  are suitably defined single-well eigenvalues. Both the diagonal and the off-diagonal elements of the diabatic potential energy matrix can then be evaluated using Eqs. (4.3) through (4.6).

The single well eigenvalues  $E_1^0$  and  $E_2^0$  in (3.7), which now define  $V_{11}$ ,  $V_{22}$  and  $V_{12}$  via Eqs. (4.3) through (4.6) are strictly defined only if the  $E_i^0$  lie below the barrier top, which seems to limit the present treatment to tunneling energies. However, the  $V^-$  in (3.7) is a very weak function of  $\rho$ , which makes it possible to simply extrapolate  $V^-$  and thus determine  $V_{11}$  and  $V_{22}$  at smaller values of  $\rho$ , where  $E_1^0$  and  $E_2^0$  are difficult to determine directly. This extrapolation enables one to extend the treatment to energies throughout one full cycle of increasing and decreasing  $P_{ij}^R$  in the transition probability  $P_{ij}^R$  vs. energy curve.

The resulting  $V_{11}$  and  $V_{12}$  versus  $\rho$  for surface IV is shown in Fig. 7 with the dashed line.  $\log V_{12}$  vs.  $\rho$  shown in Fig. 8. The right end of the curve for  $\log V_{12}$  denotes the limit of the reliability of the small numbers  $V_{12}$  obtained as a difference between two much larger numbers, (Eq. 4.5). A much more reliable treatment for this region of  $\rho$ 's (large  $\rho$ 's), based on the semiclassical treatment of a double minimum potential, is given next.

(b) Weak coupling, semiclassical evaluation of  $H_{12}$ .

The interaction matrix element  $V_{12}$  is evaluated in (4.5) from the difference between  $(W^-)^2$  and  $(V^-)^2$ , which in turn are given by differences between the two adiabatic or diabatic levels. In cases when the barrier between the two wells is very large, i.e.,  $V_{12}$  is very small, this evaluation of a small number as a difference of two large ones can, and does lead to a serious loss of accuracy. Another more direct approach to evaluating  $V_{12}$  which circumvents the above problem in the low  $V_{12}$  limit is next obtained from the semiclassical treatment of the eigenvalues of a double minimum potential.

The eigenvalues of a double minimum potential which lie below the barrier top can be obtained semiclassically by finding the energies  $E_1$  or  $E_2$  at which



the semiclassical double well eigenvalue condition (4.7) is satisfied.<sup>13,16,17</sup>

$$\tan \left[ \alpha_1(E) - \frac{\pi}{2} - \frac{\phi_1}{2} \right] \tan \left[ \alpha_2(E) - \frac{\pi}{2} - \frac{\phi_2}{2} \right] = \Gamma^2 \quad (4.7)$$

The symbols in Eq. (4.7) are given by

$$\Gamma^e(E) = \frac{e^{-2Q_i}}{1 + \sqrt{1 + e^{-2Q_i}}} \quad (4.8)$$

$$Q_i = \int_{s_2}^{s_3^i} p_i ds \quad (4.9)$$

$$\alpha_1(E_i) = \int_{s_1^i}^{s_2^i} p_i ds, \quad \alpha_2(E_i) = \int_{s_3^i}^{s_4^i} p_i ds \quad (4.10)$$

where

$$p_i = \frac{1}{\hbar} \{2[E_i - V(s; \rho)]\}^{\frac{1}{2}} \quad (4.11)$$

and the turning points  $s_j^i$  in Eqs. 4.9 and 4.10 are marked on the cut through the surface at  $\rho = \text{const.}$ , shown in Fig. 8.

On the other hand, if the wells are considered separately, one can define distorted single well eigenvalues influenced by the presence of the barrier, but for which  $\Gamma(E)$  in Eq. (4.7) is assumed, purely for this definition to be zero, i.e.,

$$\alpha_i(E_i^0) = \frac{2n_i + 1}{2}\pi + \frac{\phi}{2} \quad , \quad (4.12)$$

where  $n_i$  is the vibrational quantum number.

Since one expects that each of the two  $E_i$  would be close to the  $E_i^0$ , one can simplify Eq. (4.7) by expanding it around one of these  $E_i^0$ 's. One obtains

$$\left(\frac{d\alpha_1}{dE}\right)(E_1 - E_1^0) \tan [\alpha_2(E) - \frac{\pi}{2} - \frac{\phi}{2}] = \Gamma^2(E_1) \quad (4.13)$$

Keeping in mind that the  $E_i$  are nearly degenerate, one can further simplify (4.13) by expanding the tangent about  $E_2^0$  to get for the shift due to the presence of the other well. Thereby, we have

$$E_1 - E_1^0 = \frac{\hbar\nu_1 \hbar\nu_2}{E_2 - E_1^0} \Gamma^2(E_1) \quad (4.14)$$

where  $\nu_i$  is the local frequency, or  $\hbar\nu_i$  reciprocal density of states, given by

$$\hbar\nu_i = \frac{1}{2\pi} \frac{dE_i^0}{dn_i} \quad (4.15)$$

Similarly,

$$E_2 - E_2^0 = \frac{\hbar\nu_1 \hbar\nu_2}{E_1 - E_2^0} \Gamma^2(E_2) \quad (4.16)$$

Subtracting the two level shifts for the eigenvalues for the left and right well, and approximating  $E_i - E_j^0$  by  $\Delta E + \Delta E^0$  one gets:

$$\Delta E - \Delta E^0 = \frac{\hbar v_1 \hbar v_2}{\Delta E + \Delta E^0} \left[ \frac{\Gamma_1^2 + \Gamma_2^2}{2} \right] \quad (4.17)$$

where

$$\Delta E = \frac{1}{2} (E_2 - E_1), \quad \Delta E^0 = \frac{1}{2} (E_2^0 - E_1^0), \quad \Gamma_1 \equiv \Gamma(E_1), \quad \Gamma_2 \equiv \Gamma(E_2) \quad (4.18)$$

Identifying the difference of the two double well eigenvalues  $\Delta E$  in Eq.(4.5) with the difference of the adiabatic eigenvalues  $\epsilon^-$  and the difference of the distorted single well eigenvalues  $\Delta E^0$  with that of the diabatic eigenvalues  $V^-$  and rewriting Eq. (4.5) as

$$\Delta E - \Delta E^0 = \frac{V_{12}^2}{\Delta E + \Delta E^0} \quad (4.19)$$

and, comparing (4.16) and 4.17), one obtains

$$V_{12}^2 = \hbar v_1 \hbar v_2 \frac{\Gamma_1^2 + \Gamma_2^2}{2} \quad (4.20)$$

which in the limit of a symmetric system ( $v_1 = v_2 = v$ ,  $\Gamma_1 = \Gamma_2 = \Gamma$ ) becomes the usual degenerate level splitting result.

$$V_{12} = \hbar v \Gamma \quad (4.21)$$

The principal condition for the validity of Eq. (4.18) is the near degeneracy of the  $E_i$ , i.e., that the spacing of  $E_2$  or  $E_1$  from any other level in the system is much larger than  $E_2 - E_1$ , which is the basis of the two state approximation.

## V. EVALUATION OF THE TRANSITION PROBABILITIES

Once an approximation to the diabatic matrix elements  $V_{ij}$  has been obtained, one can, in principle, solve for the uncoupled analogs of Eq. (3.6)

$$-\frac{1}{2} \frac{d^2}{d\rho^2} \psi_i^0(\rho) = [E - V_{ii}(\rho)] \psi_i^0(\rho) \quad (5.1)$$

in order to obtain the transition probability via Eq. (3.8).

If  $V_{ii}(\rho)$  in Eq. (5.1) has no multiple turning points, a good approximation to the solution for the purpose of using it in Eq. (3.8) can be obtained by solving the equivalent of Eq. (5.1) for a potential linearized around the turning point

$$E - V_{ii}(\rho) \approx F(\rho - \rho_i) \quad (5.2)$$

where  $F = \left( \frac{dV_{ii}}{d\rho} \right)_{\rho=\rho_i}$  ( $i=1,2$ ), and  $\rho_i$  are the classical turning points.

Writing  $V_{12}$  as  $V_{12}^0 e^{-\alpha(\rho)}$  and expanding  $\alpha(\rho)$  around the outer turning point, one obtains the integral (3.8) in a form which can be evaluated analytically:

$$T_{12}^0 = \frac{2V_{12}^0}{\beta} \int_{-\infty}^{\infty} Ai[-\beta(\rho-\rho_1)] Ai[-\beta(\rho-\rho_2)] e^{-\alpha'(\rho-\rho_1)} d\rho \quad (5.3)$$

where  $\beta = (2F)^{1/3}$  and  $\alpha' = \left( \frac{d\alpha}{d\rho} \right)_{\rho=\rho_1}$

Using the integral form for the Airy functions, Eq. (5.3) transforms into

$$T_{12}^0 = \frac{V_{12}^0}{2\pi^2\beta} \int_{-\infty}^{\infty} dx \int_{-\infty}^{\infty} dy e^{i/3 (x^2 + y^2) - i\beta\Delta y} \int_{-\infty}^{\infty} d\rho e^{-i[\beta(x+y) - i\alpha]\rho} \quad (5.4)$$

where  $\Delta$  is  $\rho_2 - \rho_1$ . After some algebra, one gets

$$T_{12}^0 = \frac{V_{12}^0}{2\pi\alpha F} e^{\frac{\alpha^3}{12\beta^3} - \frac{\Delta^2\beta^3}{4\alpha}} \quad (5.5)$$

where  $V_{12}^0$  is the value of  $V_{12}(\rho)$  halfway between the turning points.

## VI. NUMERICAL RESULTS

The calculations for the nearly degenerate H-atom transfer were made on a model LEPS potential energy surface which has the asymptotic parameters for the  $\text{Cl} + \text{HBr} \rightarrow \text{ClH} + \text{Br}$  reaction. The Sato parameters were set to: 0.02, 0.02 and 0.0 in order to obtain a surface with a barrier height of  $\sim 27 \text{ kcal mole}^{-1}$ .<sup>18</sup>

The adiabatic eigenvalues  $\epsilon_i$  used to obtain  $V^+$  via Eq. (4.4) were calculated using the finite element method<sup>19</sup> used in I. The one-well eigenvalues used to obtain  $V^-$  Eq. (4.6) were obtained a) from potentials such that the potential was set to a constant equal to the barrier top energy from the barrier top into the other well, using the same method, and b) semiclassically using Eq. (4.12). The  $V^-$  was calculated only for values of  $\rho$  for which the results of a) and b) were in agreement.

$V_{12}$  was calculated from Eq. (4.5) and Eq. (4.19), respectively, in the regions of  $\rho$  noted in Fig. 8.

For surface II the nearly degenerate transition is a  $(0 \rightarrow 2)$  one. The transition probability  $P_{02}^R$  was evaluated using Eq. (5.1) and is given on Fig. 9 as a function of the energy. The log of the transition probability  $P_{02}^R$  vs. energy in the tunneling region is given in Fig. 10.

## REFERENCES

1. V. K. Babamov and R. A. Marcus, J. Chem. Phys., 74, 1790 (1981).
2. A. Kuppermann, J. A. Kaye and J. P. Dwyer, Chem. Phys. Lett., 74, 257 (1980).
3. J. A. Kaye and A. Kuppermann, Chem. Phys. Lett., 77, 573 (1981).
4. J. Manz and J. Rommelt, Chem. Phys. Lett., 81, 179 (1981)
5. The shift reported in ref. 3, 1.38 mev ( $3.2 \times 10^{-3}$  kcal) (Table II, surface A in ref. 3), contained an error.
6. We were only able to make a comparison of this precision with ref. 3 by using the eigenvalues obtained in ref. 3. Even the the IHI case two calculations from different laboratories are likely to differ more than the shift observed, due to slight differences in the masses, physical constants or numerical techniques used.
7. The  $\eta(s;p)$  are a set of orthogonal vibration states which retain the configuration of either the reactants or the products and at large reduce to either the reactants or the products asymptotic states.
8. F. T. Smith, Phys. Rev., 179, 111 (1969); V. K. Babamov, J. Chem. Phys., 69, 3414 (1979).
9. E. g., M. S. Child, Molecular Collision Theory (Academic Press, NY, 1974).
10. T. Uzer and M. S. Child, Molec. Phys., 41, 1177 (1980).
11. R. D. Levine, Molec. Phys., 22, 497 (1971).
12. The parameters are the same as those of ref. 3, except for the Sato parameter which has been set equal to zero.
13. J. N. L. Connor, Chem. Phys. Lett., 4, 419 (1969).
14. D. R. Bates and R. McCarroll, Proc. Roy. Soc. London A245, 175 (1958);  
A. Riera and A. Salin, J. Phys. B: Atom. Molec. Phys., 9, 2877 (1976).

15. W. R. Thorson and J. B. Delos, Phys. Rev., A18, 135 (1978); L. F. Errea, L. Mendez and A. Riera, J. Phys. B, 15, 101 (1982).
16. N. Froman, Arkiv. Rysik, 32, 79 (1966).
17. W. H. Miller, J. Phys. Chem., 83, 960 (1979).
18. The Sato parameter was reduced, to obtain a higher barrier on the surface and make the  $V_{ij}$  in Eq. (5.1) monotonic functions of  $\rho$ . If the  $V_{ij}$  have wells, which is the case for H-atom transfer reactions with very low barriers one must evaluate the integral (3.8) numerically.
19. D. J. Malik, J. Eccles and D. Secrest, J. Comput. Phys., 38, 157 (1980).

## FIGURE CAPTIONS

- Figure 1. Ground vibrational state transition probability for the  $IH + I \rightarrow I + HI$  reaction. The solid line is the result of Eq. (2.3) and the circles are the accurate numerical results of ref. 3.
- Figure 2. Ground vibrational state transition probability for the model<sup>12</sup> surface I. The solid line is the exact solution of Eq. (2.2) given by Eq. (2.3) and the circles are the result of the present exponential DWBA approximation (Eq. 3.10). The dotted line is the DWBA without the exponential approximation.
- Figure 3. The logarithm of the transition probability vs. energy for surface I. The solid line is the result of Eq. (2.3) and the circles are the present result (Eq 3.10).
- Figure 4. Contour plot for the surface I<sup>12</sup>.
- Figure 5. Contour plot of the surface II<sup>19</sup>. The contour energies are in kcal mole<sup>-1</sup>.
- Figure 6. A cut through model surface II at  $\rho = \text{const.}$  The solid horizontal lines show the adiabatic levels and the dashed ones the diabatic levels. The  $s_i^1$  in the figure are the integration limits for Eqs. (4.9) and (4.10) for  $E = E_1$ .
- Figure 7. Diagonal adiabatic (dashed line) and diabatic (full line) matrix



elements for model II. ( $\text{Cl} + \text{HBr} \rightarrow \text{ClH} + \text{Br}$ )

Figure 8. The log at  $\text{H}_{12}$  vs.  $\rho$  for model surface II. The dashed part of the curve corresponds to the region where Eq. (4.5) becomes unreliable. ( $\text{Cl} + \text{HBr} \rightarrow \text{ClH} + \text{Br}$ )

Figure 9. The transition probability vs. energy (Eq. 5.5) for the model surface II. ( $\text{Cl} + \text{HBr} \rightarrow \text{ClH} + \text{Br}$ )

Figure 10. The log of the transition probability for surface II in the tunneling region.

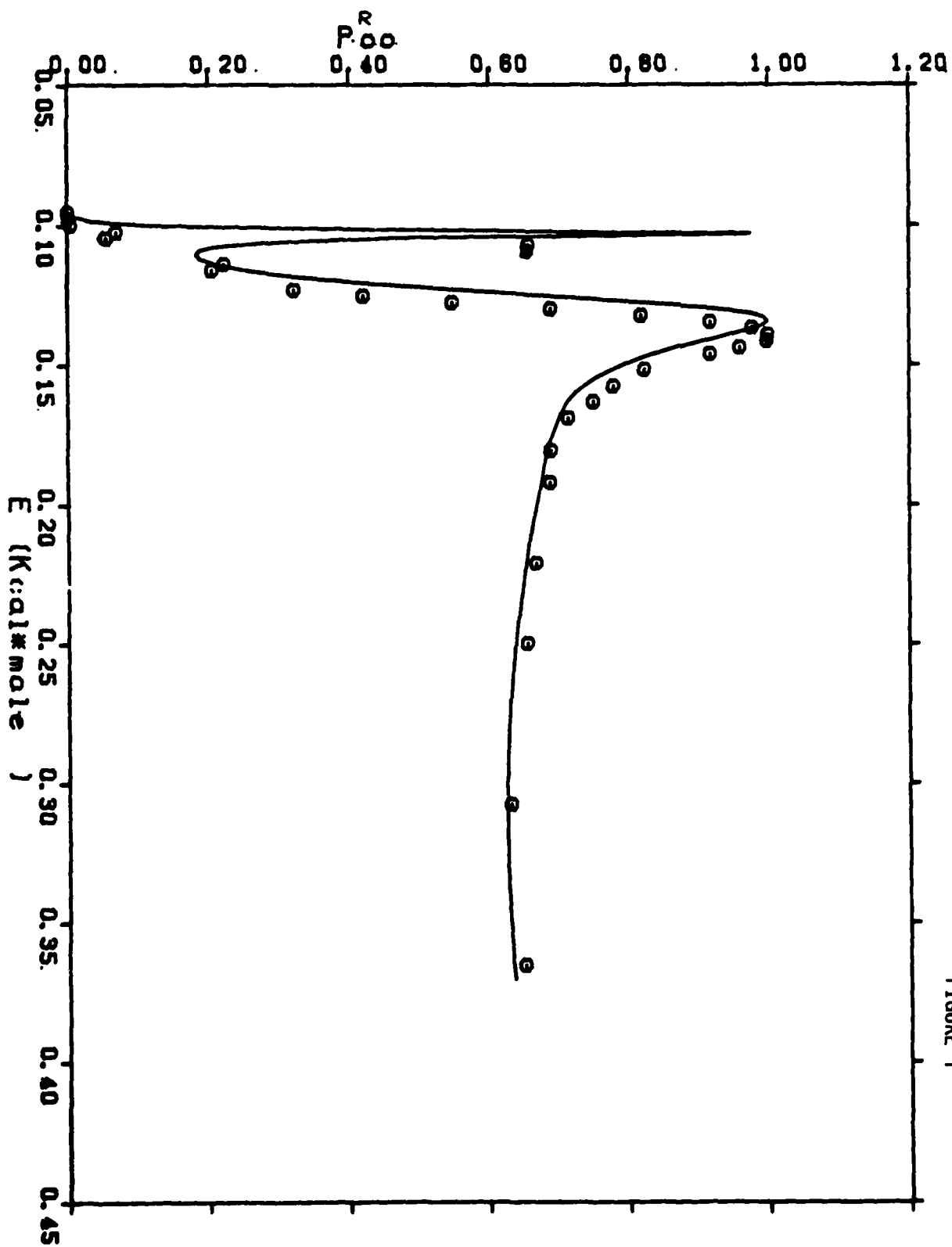


FIGURE 1

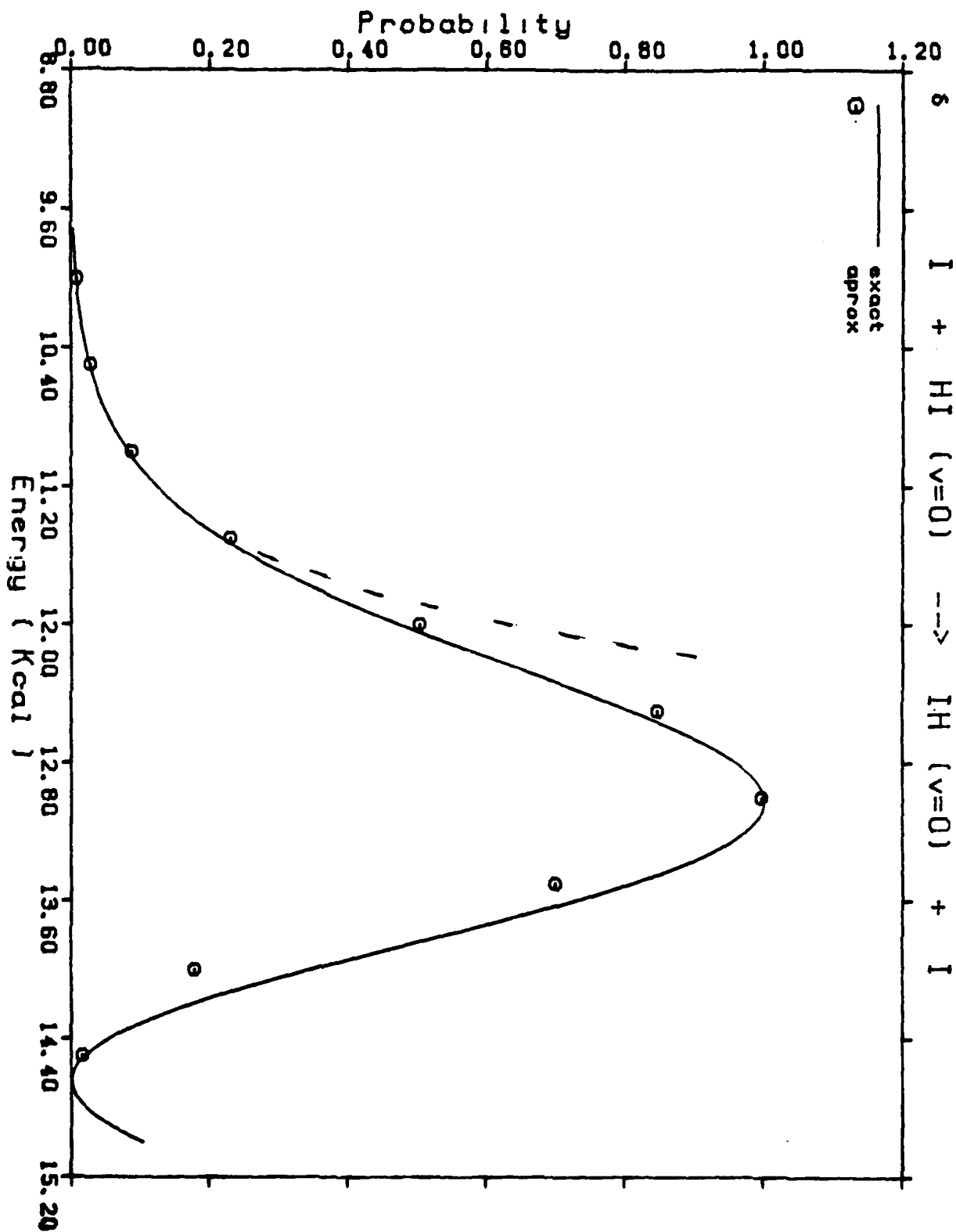
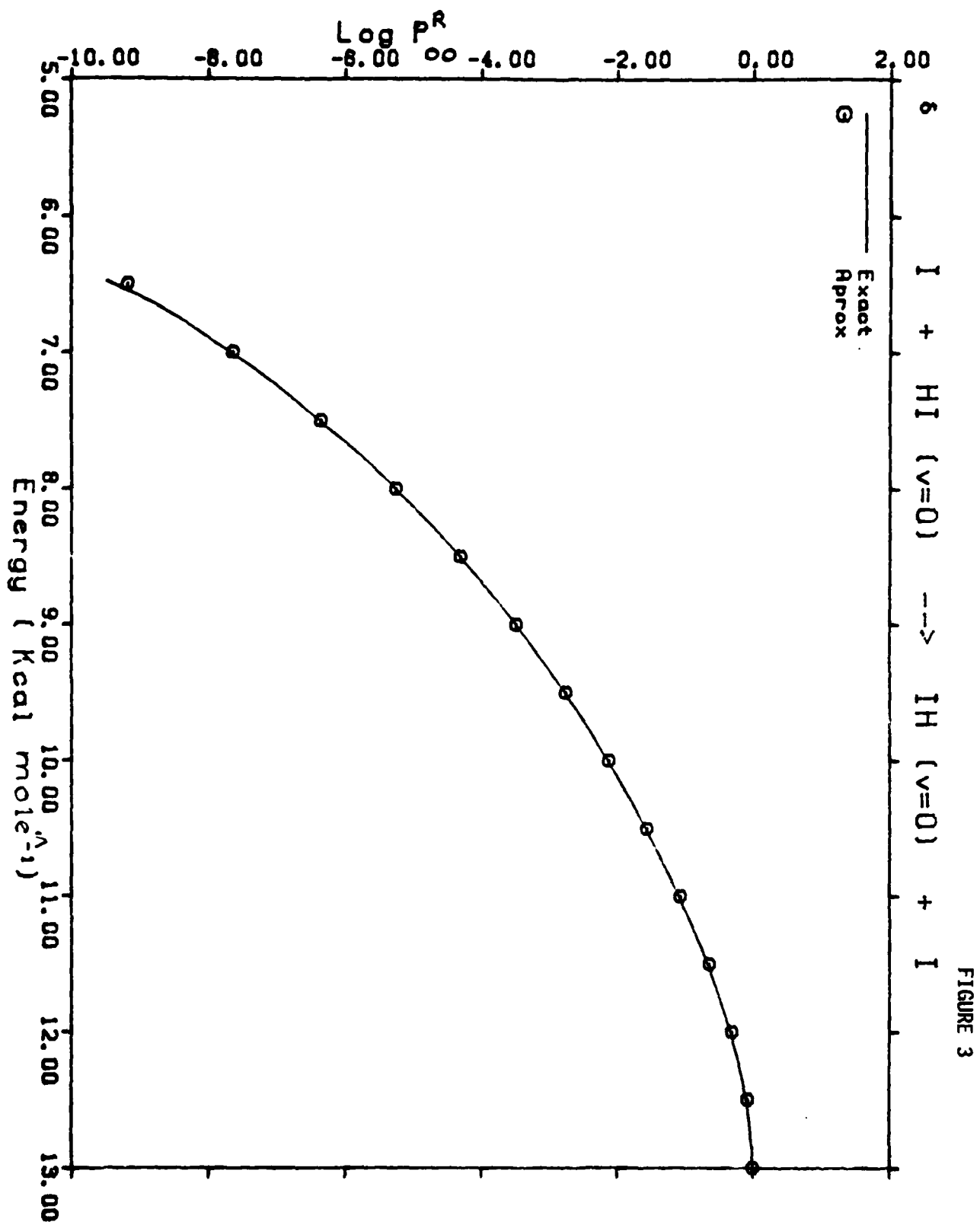


FIGURE 2



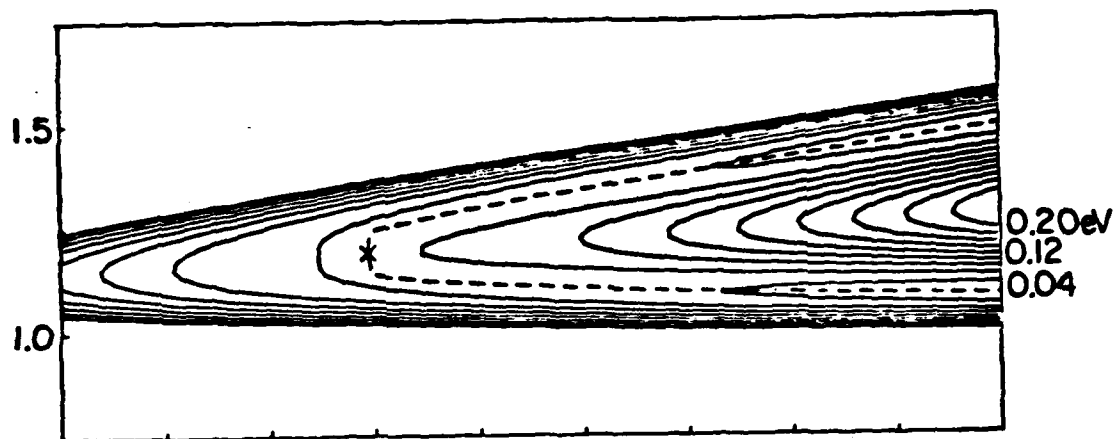


FIGURE 4

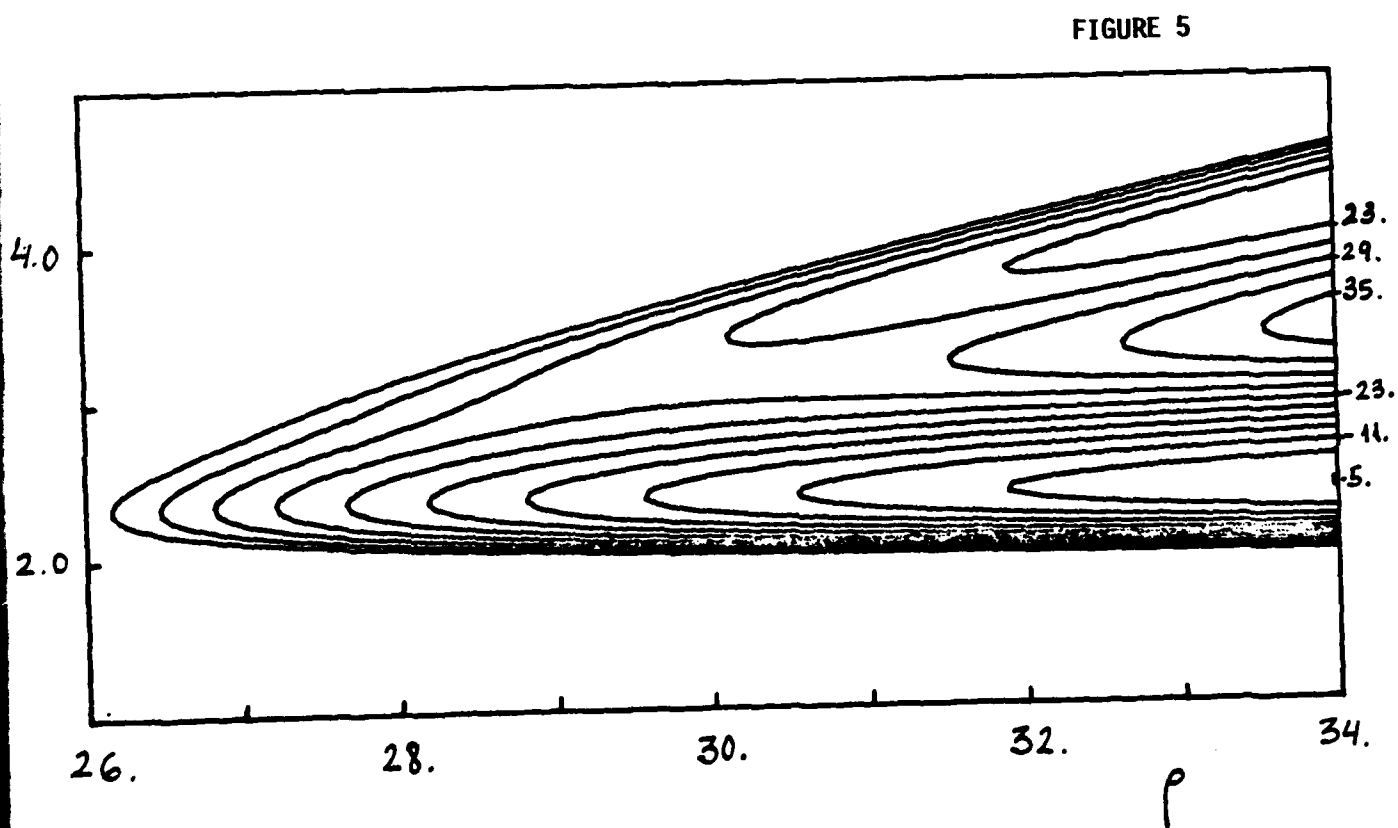
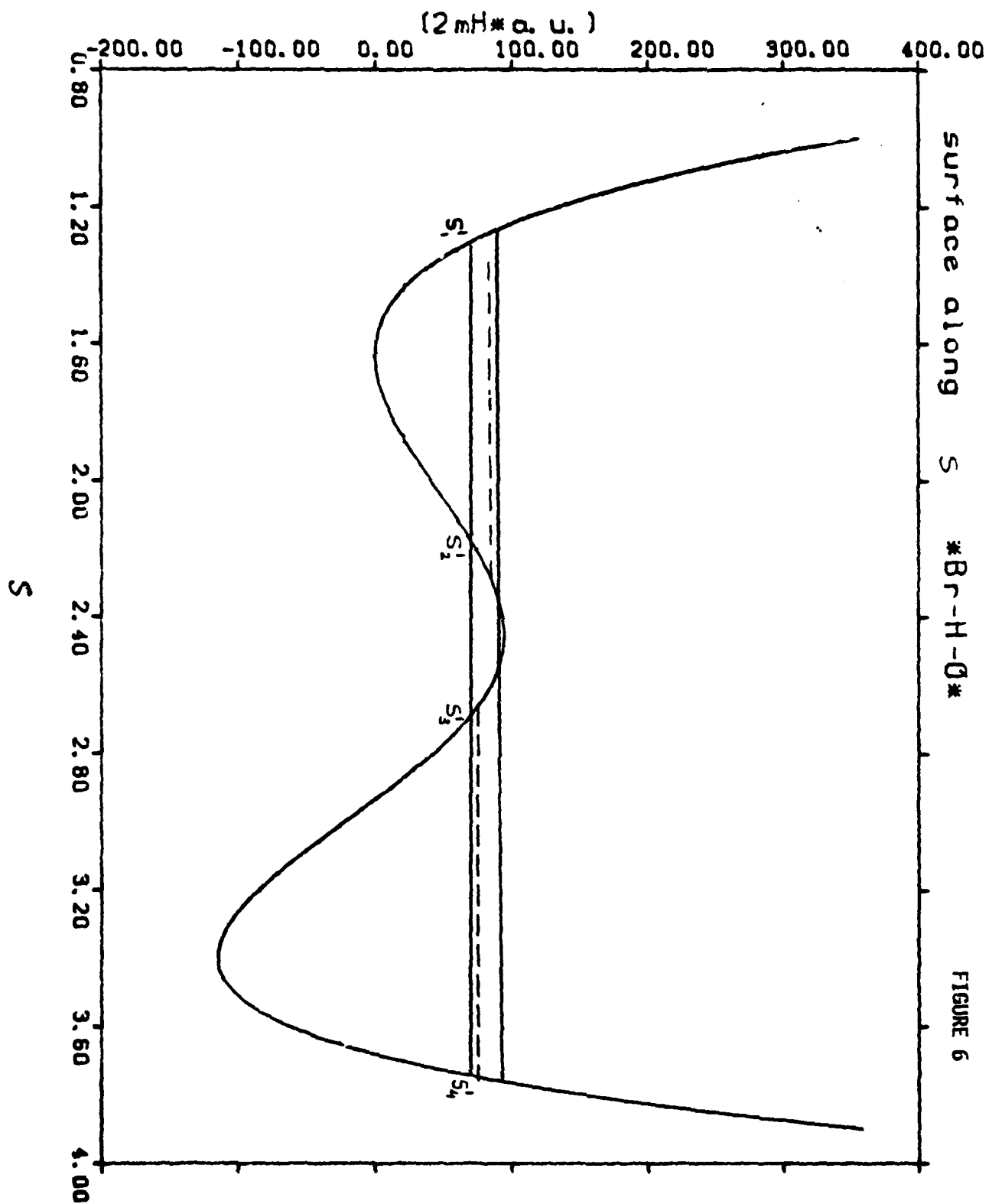


FIGURE 5



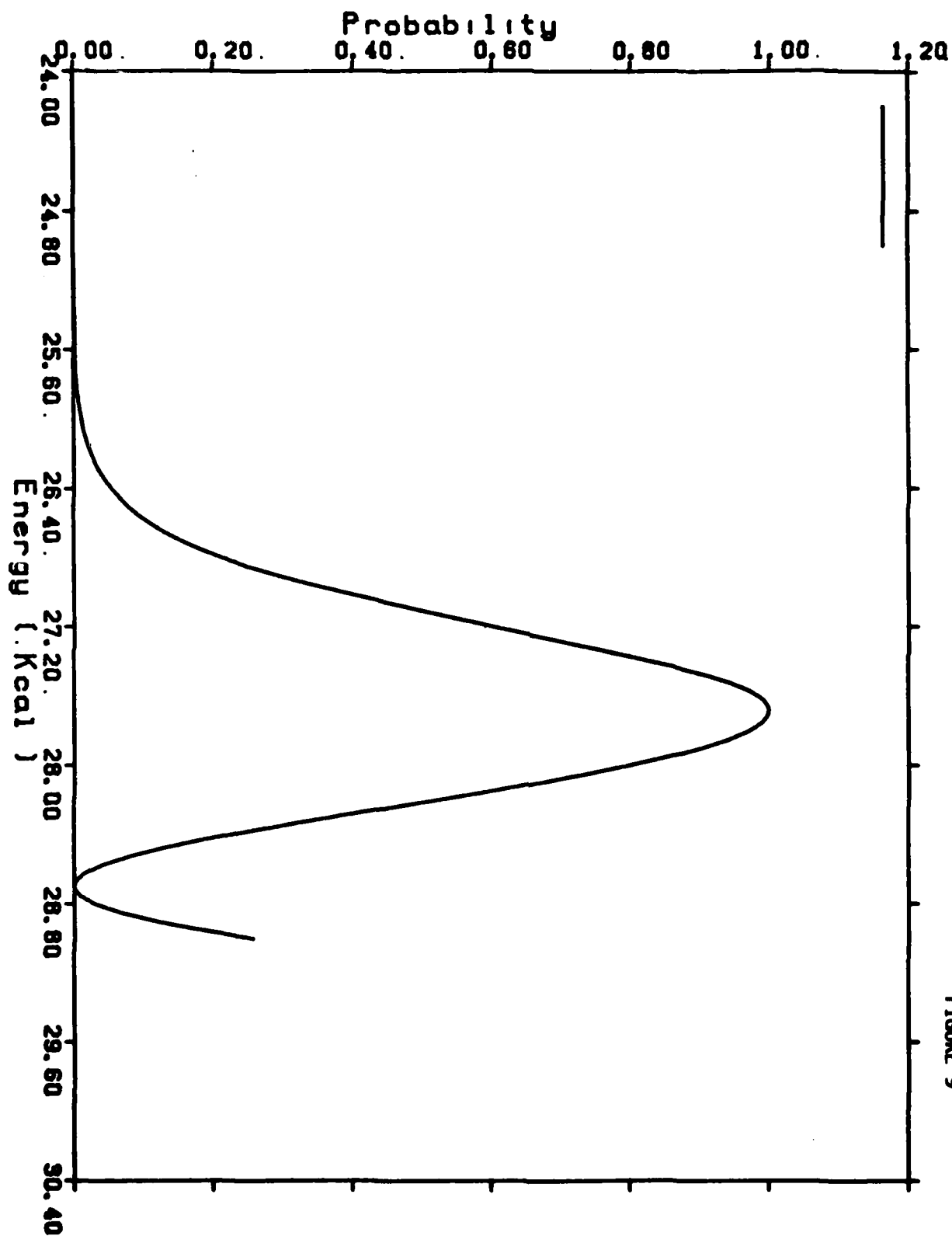


FIGURE 9

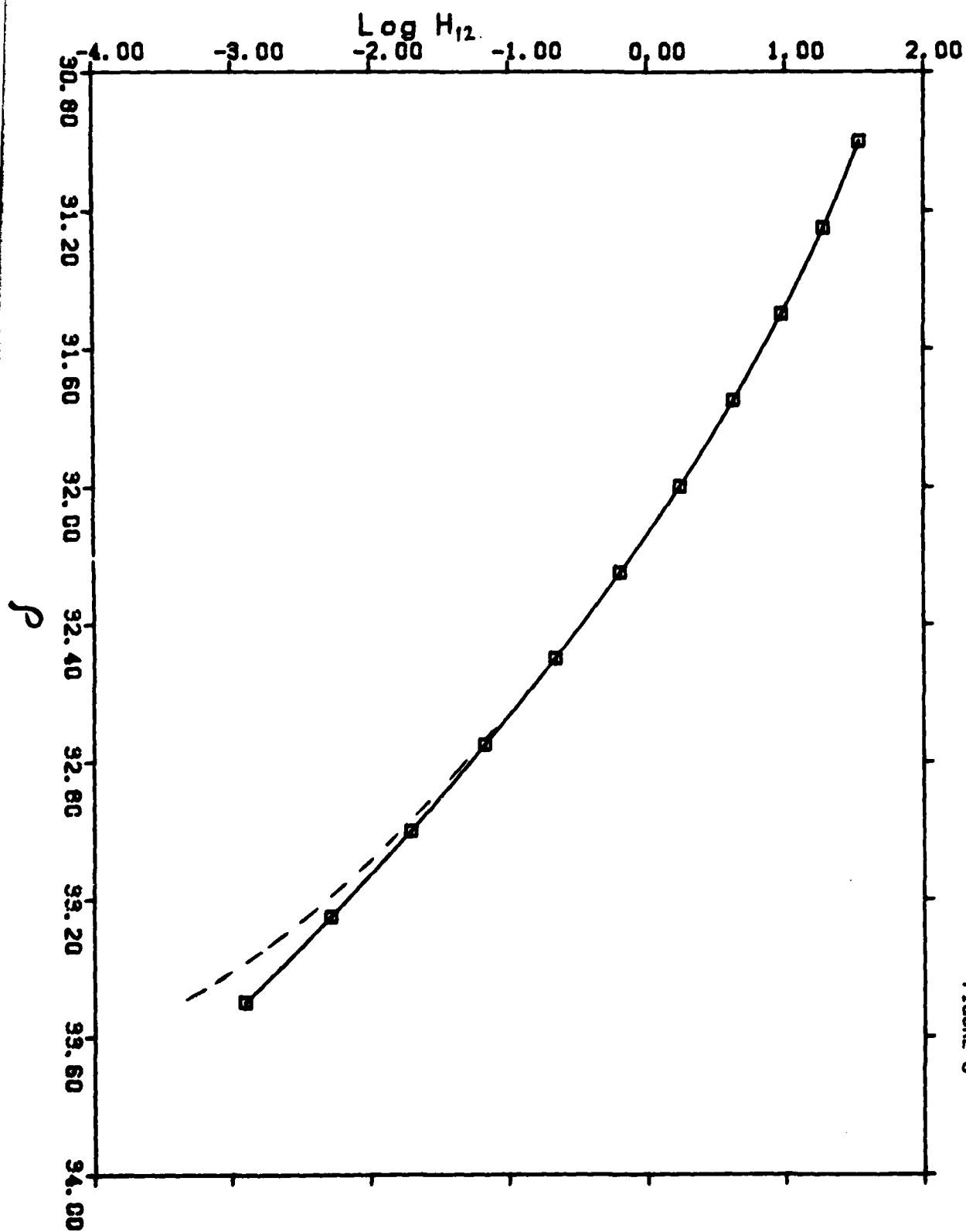


FIGURE 8



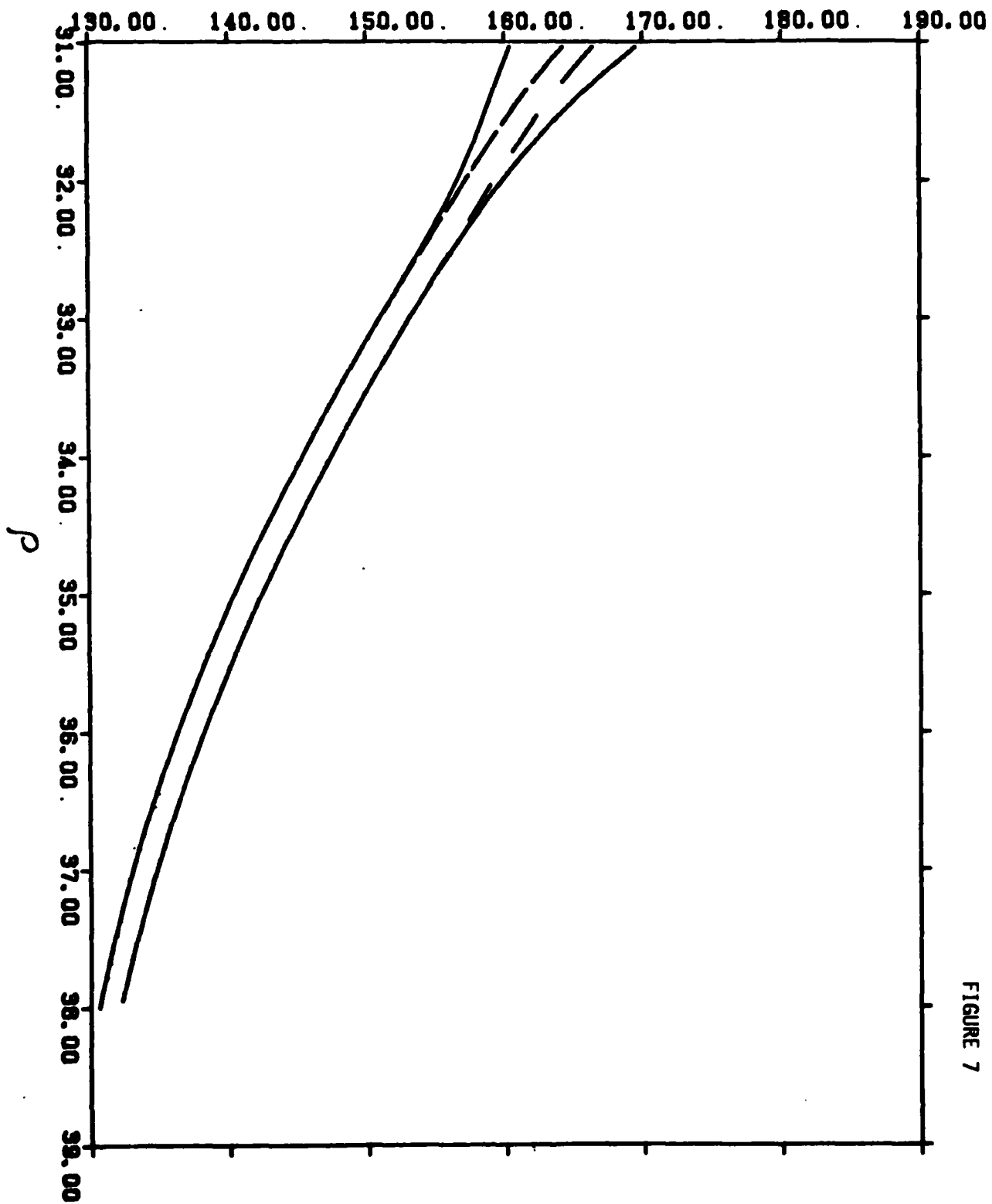


FIGURE 7

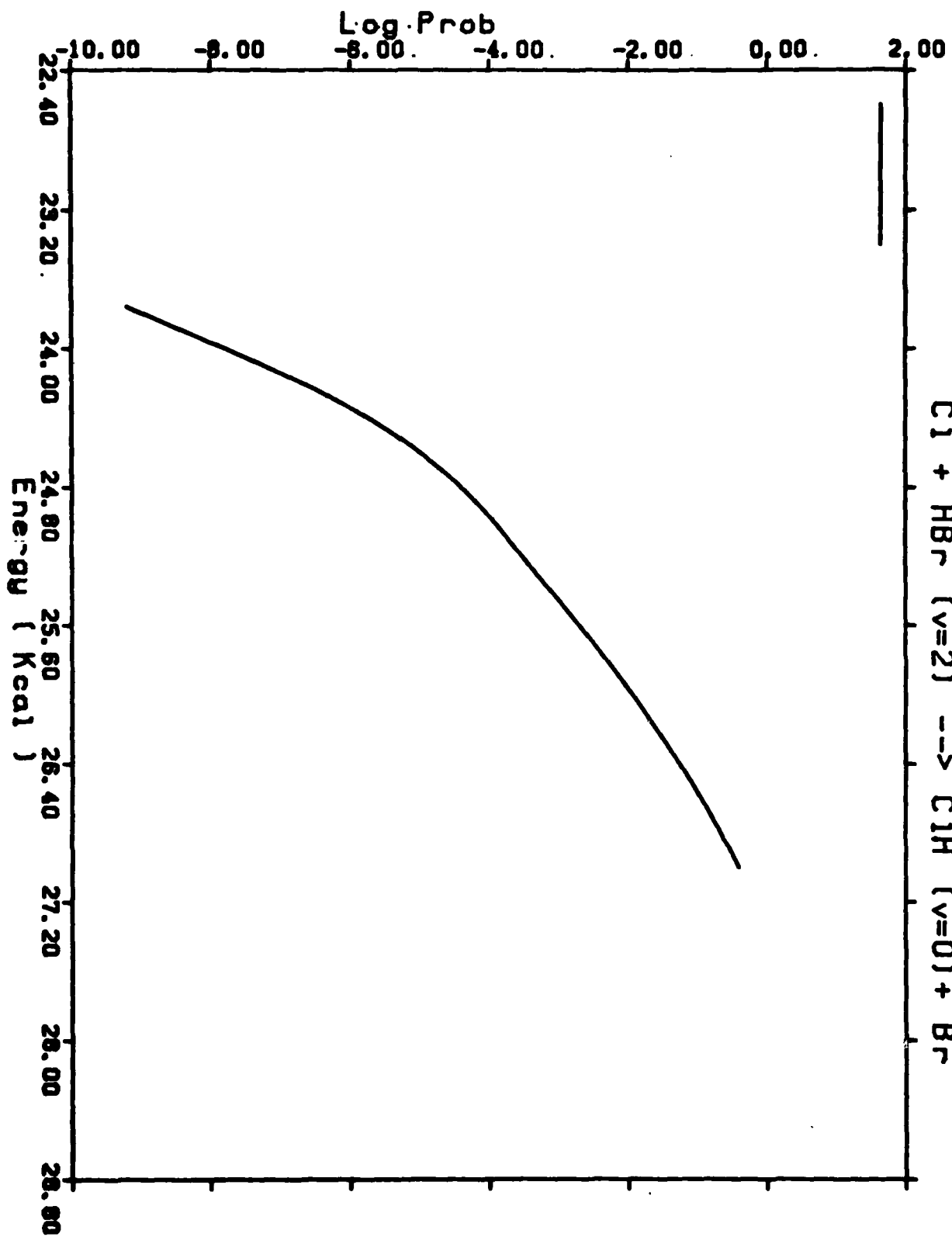


FIGURE 10

ATE  
MED  
-8